Analysis and Comparison of Extremum Seeking Control Techniques

Carlos Olalla, Maria Isabel Arteaga, Ramon Leyva, Abdelali El Aroudi
Departament d'Enginyeria Electrònica, Elèctrica i Automàtica
Universitat Rovira i Virgili
Tarragona, Spain
Email: carlos.olalla@urv.cat, mariaisabel.arteaga@urv.cat, ramon.leyva@urv.cat, abdelali.elaroudi@urv.cat

***Abstract*— Two non-perturvative extremum seeking control approaches are analyzed; the first approach needs the sensing of the function's gradient while the second one does not. Relationships between the algorithms parameters and their dynamic behavior are found. Also expressions for the steady state error of both approaches are derived. Finally, these results are used to verify and to compare, by means of simulation, the performance of both methods.**

I. Introduction

Extremum Seeking Control (ESC) considers the problem of tracking an input x which optimizes an unknown and usually time-variant function $y(x)$,

$$x^* = arg\ max_{x \in \mathbf{R}}\ y(x) \tag{1}$$

or also

$$x^* = arg\ min_{x \in \mathbf{R}}\ y(x) \tag{2}$$

where x^* is the argument which maximizes or minimizes the function $y(x)$. It is assumed that there only exist a single maximum or minimum point in $y(x)$, i.e. that $y(x)$ is concave or convex.

Since the original work from Leblanc [1], ESC has been subject of numerous researches. Reference [2] differentiated between ESC methods which require an external perturbation of the input variable (also known as *perturb and observe*) [3], [4], and ESC methods which do not require an external perturbation [5], [6], [7] and [8].

The present work considers the algorithms which do not need the external perturbation signal, and states the differences between two of them. Reference [6] is one of the best known algorithms in the field of Maximum Power Point Tracking (MPPT). It requires sensing the function gradient to switch a relay which sets the direction to the optimum point; the algorithm is usually called *relay ESC*. Gradient sensors (or differentiators) tend to amplify noise and suffer from instability problems at high frequencies. Usually the differentiator only acts for a short known safe bandwidth, which constraints the dinamic performance of the sensor. Nevertheless, references [7] and [8] do not sense the output gradient and are based in the introduction of Sliding Modes (SM); we will refer to them as *SM ESC*.

Both approaches will be analyzed and simulated in order to seek the maximum point ($y(x)$ is assumed to be concave) of a function which is similar to the output power of a solar panel array, and therefore the results could be applied to MPPT systems (See fig. 1).

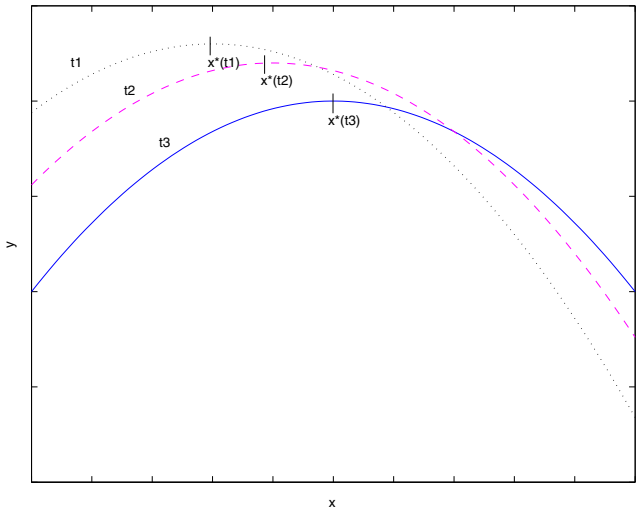

Fig. 1. Time-variant concave function $y(x)$ for different time values.

This work is organized as follows. Section II shows a detailed analysis which results in relationships between the system parameters and its dynamic behavior. Section III verifies the results to set up and compare the algorithms by means of simulation. Section IV presents the performance differences between both methods and gives some conclusions.

II. ESC Working Principle Analysis

This section analyzes the relay ESC and the SM ESC shown in [5], [6] and [7], [8] respectively.

For both approaches there exist algorithms using constant and non constant seeking ratio. In this work we consider constant seeking ratio.

A. Relay ESC

Relay ESC systems change the direction of the seeking input depending on the sign of the gradient dy/dx, that is obtained from the derivative

$$g = dy/dt. \tag{3}$$

Fig. 2, which has been adapted from [6], shows the block diagram of a relay ESC system. Note the gradient detector

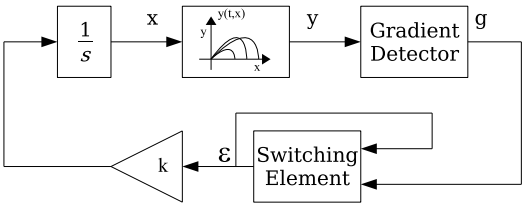

Fig. 2. Block diagram of the relay ESC algorithm.

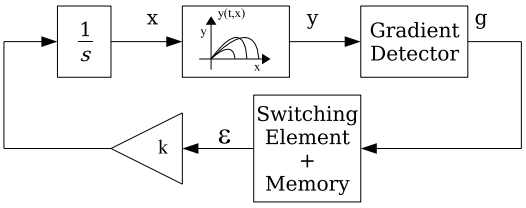

Fig. 3. Block diagram of the relay ESC algorithm with memory.

$g = dy/dt$ and the actuator, where the relay is located and whose response is described by

$$\begin{cases} \epsilon = +1 & \text{if } sign\left(\frac{dy}{dt}\right) \cdot sign\left(\frac{dx}{dt}\right) > 0 \\ \epsilon = -1 & \text{if } sign\left(\frac{dy}{dt}\right) \cdot sign\left(\frac{dx}{dt}\right) < 0\ . \end{cases} \tag{4}$$

We can describe the dynamic behavior of the state variable x as follows

$$\frac{dx}{dt} = k \cdot \epsilon = k \cdot sign\left(\frac{dy}{dt}\right) \cdot sign\left(\frac{dx}{dt}\right), \tag{5}$$

where

$$sign\left(\frac{dy}{dt}\right) = sign\left(\frac{dy}{dx}\right) \cdot \left(\frac{dx}{dt}\right). \tag{6}$$

Expression (5) can be simplified using (6) as follows

$$\frac{dx}{dt} = k \cdot sign\left(\frac{dy}{dx}\right). \tag{7}$$

An equivalent algorithm can be also implemented using a memory element by

$$\begin{cases} \text{if } dy/dt > 0 & \text{Keep the sign of } \epsilon \\ \text{if } dy/dt < 0 & \text{Change the sign of } \epsilon. \end{cases} \tag{8}$$

The memory can be implemented with a latch and the resulting block diagram is shown in Fig. 3

In [6] it is demonstrated that the algorithm is stable for a concave function and that the input x converges to x^* with a slope k. Once the algorithm reaches the optimum point its control variable ϵ switches at a very high frequency. To limit the relay switching frequency several strategies have been show in the literature.

1) To include a hysteresis in the control law as follows

$$\begin{cases} \text{if } dy/dt - \Delta > 0 & \text{Keep the sign of } \epsilon \\ \text{if } dy/dt + \Delta < 0 & \text{Change the sign of } \epsilon. \end{cases} \tag{9}$$

Note that the switching frequency depends on k, Δ and the function to optimize. The maximum error to the optimum point depends on Δ.

2) To include a constant delay T_d to maintain the sign of ϵ for a minimum time. The parameters to set up in the algorithm are T_d and k. The switching frequency is defined by

$$f_{relay} = \frac{1}{2 \cdot T_d}, \tag{10}$$

and the maximum error between x and x^* is found to be

$$e_{relay} = k \cdot T_d, \tag{11}$$

B. Sliding Mode ESC

Sliding Mode (SM) ESC block diagram has been depicted in fig. 4, extracted from [8]. The main advantage of this ESC algorithm is that it does not require gradient sensors. The behavior of the block diagram is described by

$$u = dx/dt \tag{12}$$

$$u = U_0\ sign(\sigma_1 \sigma_2) \tag{13}$$

$$\sigma_1 = \epsilon \tag{14}$$

$$\sigma_2 = \epsilon + \delta \tag{15}$$

$$\epsilon = g - y \tag{16}$$

$$dg/dt = \rho + M\upsilon(\sigma_1,\ \sigma_2) \tag{17}$$

where U_0, δ, ρ, M are positive constants and υ is a three states function of σ_1 and σ_1 as is depicted in fig. 5.

If the following inequality holds

$$M > U_0 \left|\frac{df}{dx}\right| + \rho, \tag{18}$$

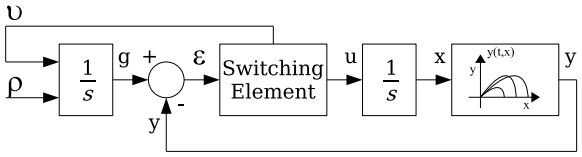

Fig. 4. Block diagram of the Sliding Mode ESC algorithm.

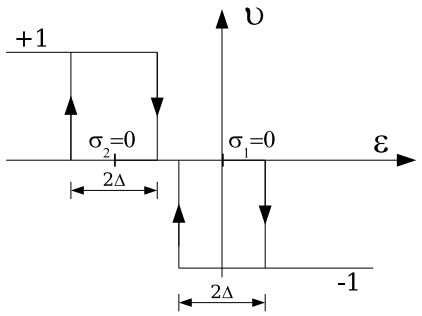

Fig. 5. Function of the switching element $\upsilon(\sigma_1\sigma_2)$.

then, assuming the initial state $(\sigma_1 - \Delta)(\sigma_2 + \Delta) > 0$, the change of σ_1 and σ_2 is

$$\dot{\sigma_1} = \dot{\sigma_2} = \frac{df}{dx} U_0 + \rho + M\upsilon. \tag{19}$$

Thanks to (19), g reaches a value close to y where $(\sigma_1 - \Delta)(\sigma_2 + \Delta) < 0$ and $\upsilon = 0$. The required time to reach this second state is easily reduced by enlarging M. Once $\upsilon = 0$, the change ratio of σ_1 and σ_2 is

$$\dot{\sigma_1} = \dot{\sigma_2} = \rho - \frac{df}{dx} U_0 sign(\sigma_1 \sigma_2), \tag{20}$$

while the following condition holds

$$\left| \frac{df}{dx} \right| U_0 > \rho. \tag{21}$$

In this second state ($\upsilon = 0$), depending on the sign of df/dx, σ_1 or σ_2 will tend to zero, because in this state their sign is opposite. Furthermore, any change in the sign of σ_1 or σ_2 changes the sign of its derivative, and therefore a sliding mode is originated in the system. In an ideal framework, u switches at infinite frequency and the value of σ_1 or σ_2 is zero. If $\upsilon = 0$ then we can state that the reference g increases monotonically with ratio ρ and therefore we can say that y follows the increasing reference, since

$$\sigma_1 = g - y \approx 0, \tag{22}$$

$$\sigma_2 = g - y + \delta \approx 0. \tag{23}$$

Therefore the output y increases to a certain point close to the maximum, where (21) does not hold.

In this third state the output y does not increase monotonically with ρ, and (23)(22) is not true anymore. However, υ maintains σ_1 and σ_2 inside the range $\sigma_1 < \Delta$ and $\sigma_2 > -\Delta$. Hence it has been demonstrated that the input x is keeps close to the maximum point x^*.

In [7] it is shown that under these conditions σ_1 or σ_2 reaches $+\Delta$ or $-\Delta$ during t_1 and t_2, which are defined by

$$t_1 = \frac{\Delta}{\rho - U_0 \frac{df}{dx}}, \tag{24}$$

$$t_2 = \frac{\Delta}{\rho + U_0 \frac{df}{dx}}. \tag{25}$$

If we assume that $\rho \gg U_0 \left| df/dx \right|$ in the vicinity of x^*, then the time period is described by

$$t_{12} = t_1 + t_2 = \frac{2\Delta}{\rho}. \tag{26}$$

If we approximate (20) by

$$\dot{\sigma_1} = \dot{\sigma_2} = \rho, \tag{27}$$

then σ_1 (or σ_2) will reach $+\Delta$ (or $-\Delta$) at the time t_{12}, when υ will be again different from zero and σ_1 will return to $+\Delta$ in a time close to zero, as M is very large.

Therefore we can consider that when x is close to x^* there exist a sliding mode whose switching frequency is

$$f_{sm} = \frac{\rho}{2\Delta}, \tag{28}$$

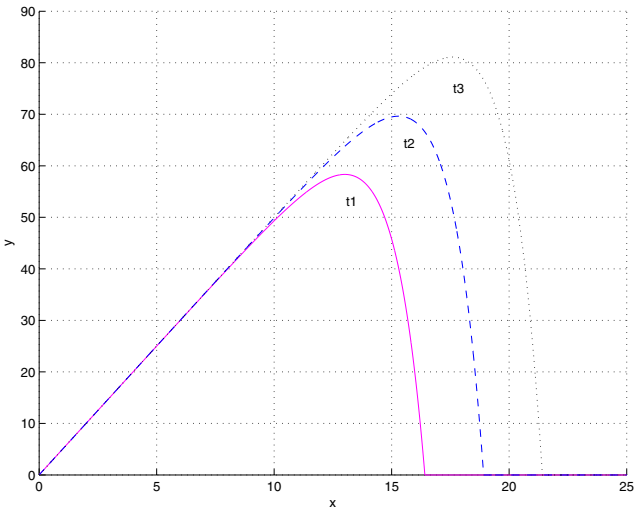

Fig. 6. Time-variant $y = f(x)$ used for simulation.

and that the maximum error between x and x^* is

$$e_{sm} = \frac{\Delta}{2\rho} U_0, \tag{29}$$

The required parameters to set up the SM ESC algorithm are Δ, δ, M, U_0 and ρ. Note that the following relationships must hold,

$$\Delta < \delta, \tag{30}$$

$$M \gg U_0, \tag{31}$$

$$M \gg \rho, \tag{32}$$

in other words, U_0 must be chosen sufficiently large to meet (21) and sufficiently small to meet (23).

III. Simulation Results

In the previous section we have derived the steady state switching frequency and error of the two ESC algorithms of interest. Now we will fix a switching frequency of 10 kHz to set up the simulation and to compare the performance of the methods.

The objective function to optimize is shown in fig. 6. Its response is very similar to the one that could be found in a power limited current source, having a variable power limit. These are the usual conditions in photovoltaic applications and therefore the work could be ported to MPPT systems.

A. Relay ESC

We set a relay ESC system with constant seeking slope k and delay time T_d. If we desire a steady state switching frequency of 10 kHz, then

$$T_d = 50\mu s. \tag{33}$$

At the same time, if we consider that the minimum value of the input x is $x_{min} = 10$, then we can set a maximum steady state error of 0.1% as follows

$$K = \frac{T_d}{e_{relay}} = 200. \tag{34}$$

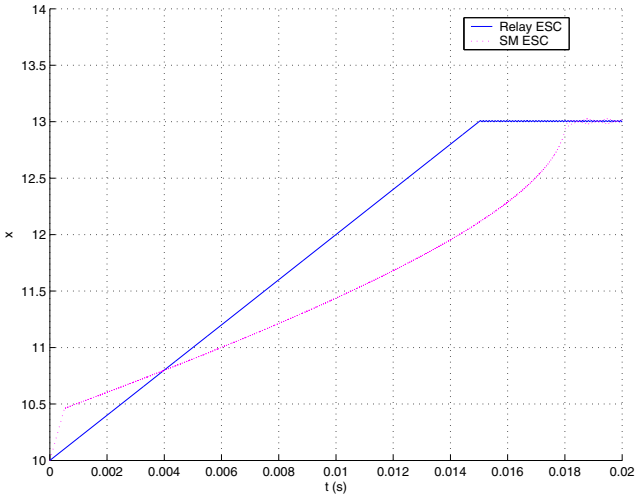

Fig. 7. Seeking transient for $x_0 < x^*$.

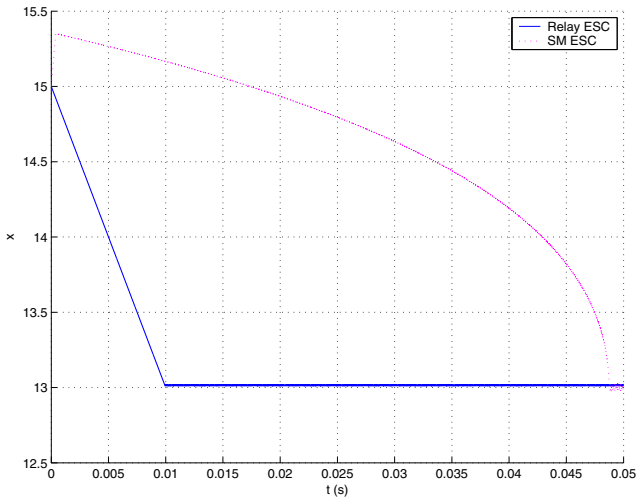

Fig. 8. Seeking transient for $x_0 > x^*$.

B. Sliding Mode ESC

For the SM ESC, we must fulfill $\Delta < \delta$

$$\Delta = 0.02, \qquad \delta = 0.05 \tag{35}$$

Using (28) we meet the steady state switching frequency

$$\rho = 400. \tag{36}$$

Then we choose $M \gg \rho$

$$M = 1 \cdot 10^5. \tag{37}$$

Finally we must fulfill (21) and (23)

$$U_0 = 900, \tag{38}$$

which yields a steady state error of

$$e_{SM} = 0.0225 \quad \rightarrow \quad \approx 0.2\% \tag{39}$$

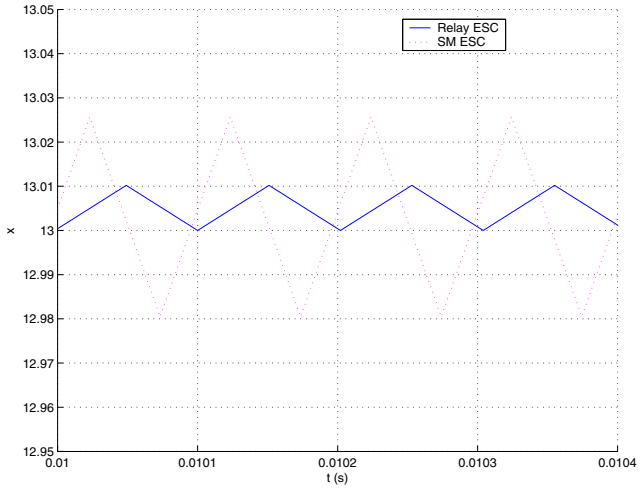

Fig. 9. Steady state error.

C. Results

Fig. 7 shows the transient response when the initial condition of x is $x_0 < x^*$. Similarly, fig. 8 shows the transient when $x_0 > x^*$.

The steady state error has been depicted in fig. 9. Note that the switching frequency is equal in both cases.

Finally, figs. 10, 11 and 12 show the transient response to changes in $f(x)$. Fig. 10 shows the response to step changes in the maximum power point. Fig. 11 shows the transient when the maximum power point increases with a constant slope and fig. 12 shows a $x - y$ detail under these conditions.

From the simulation results we conclude that

1) Due to the working principle of the SM ESC, it is configured to run in a single direction (up or down) depending on ρ, and its performance is degraded when it runs in the opposite direction.
2) In the SM ESC, the slope of the input signal increases as df/dx decreases, while the slope is constant in the relay ESC.

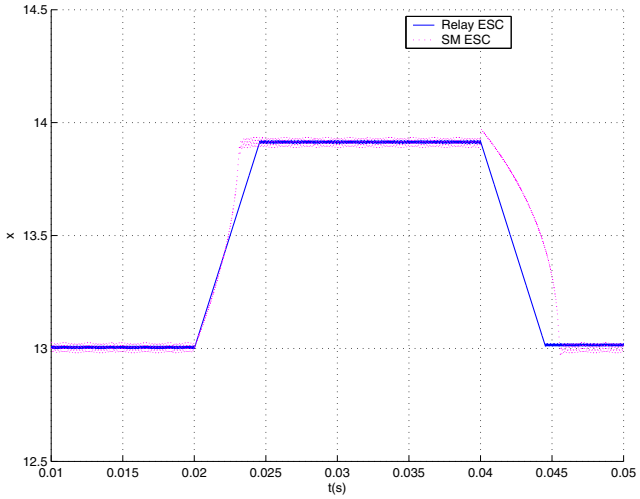

Fig. 10. Seeking transient for a step perturbation.

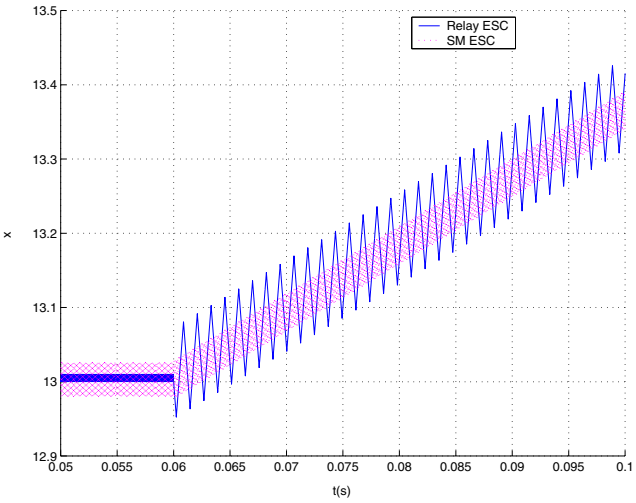

Fig. 11. Seeking transient for a ramp perturbation.

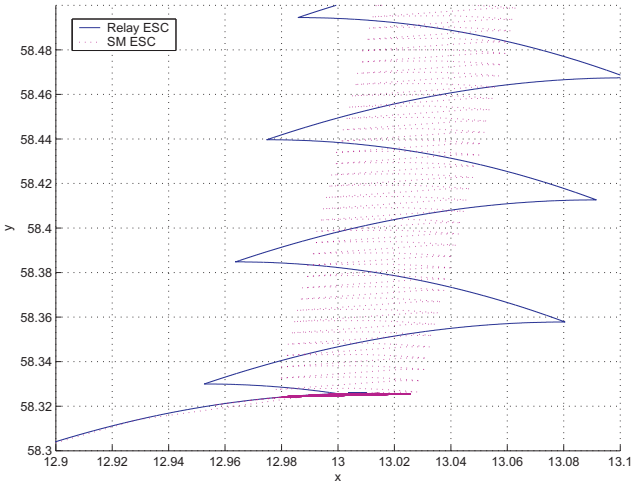

Fig. 12. x-y detail of the seeking transient for a ramp perturbation.

3) Due to the previous facts, the relay ESC performance is better for the initial transient, when the initial conditions are far from the maximum point.
4) The relay ESC steady state error is lower than the observed in the SM ESC.
5) The SM ESC is able to track the ramp perturbation, maintaining the error close to the steady state value. However the relay ESC shows larger oscillations when the perturbation appears. This is due to the fact that the gradient detector can show positive readings when the maximum power point is moved, despite that the gradient of $f(x)$ may be negative.

IV. Conclusions

This paper showed 2 non-perturbative ESC techniques and compared their performance for the same switching frequency. We observed that the relay ESC has lower steady state error and better performance under the initial conditions. Also the relay ESC showed large oscillations for changes in the maximum point, due to the gradient detector limitations. On the other hand, we observed that the SM ESC has the same steady state error during the ramp perturbation. However there are not *significant* differences and both methods are very similar in terms of performance.

The implementation of the SM ESC is constructed with a larger number of relays and integrators, but it does not require a differentiator to sense the gradient. Nevertheless the relay ESC block diagram is simpler, but it requires a differentiator, which may present several difficulties. Therefore SM ESC are a suitable alternative to avoid the use of differentiators in MPPT applications.

References

[1] M. Leblanc, "Sur la electrification des chemins de fer au moyen de coraunts alternatif de frequence elevee," *Revue Generale de l'Electricite*, vol. XII, pp. 275–277, 1922.
[2] I. S. Morosanov, "Methods of extremum control," *Automatic and Remote Control*, vol. 18, pp. 1077–1092, 1957.
[3] M. Krstic and H. Wang, "Design and stability analysis of extremum seeking feedback for general nonlinear systems," in *Decision and control, Proceedings of the 36th IEEE Conference*, 1997.
[4] M. Krstic and K. B. Ariyur, *Real Time Optimization by Extremum Seeking Control*. Wiley Interscience, 2003.
[5] J. L. Abatut, "Etude de rergulation extremale en vue notamment de l'optimization d'une unité industrialle de reforming catalytique," Ph.D. dissertation, Université de Toulouse, 1965.
[6] R. Leyva, C. Alonso, I. Queinnec, A. Cid-Pastor, D. Lagrange, and L. Martinez-Salamero, "Mppt of photovoltaic systems using extremum - seeking control," *Aerospace and Electronic Systems, IEEE Transactions on*, vol. 42, no. 1, pp. 249–258, 2006, 0018-9251.
[7] S. K. Korovin and V. I. Utkin, "The use of the slip mode in problems of static optimization," *Automatic and Remote Control*, pp. 50–60, 1972.
[8] S. K. Korovin and V. I. Utkin, "Using sliding modes in static optimization and nonlinear programming," *Automatica*, vol. 10, pp. 525–532, 1974.